Theoretical study of excitation of the low-lying electronic states of water by electron impact

T. N. Rescigno[1] and A. E. Orel[2]

[1]*Lawrence Berkeley National Laboratory, Chemical Sciences, Berkeley, California 94720, USA*

[2]*Department of Chemical Engineering and Materials Science, University of California, Davis, California 95616, USA*

(Received 20 May 2013; published 8 July 2013)

We report the results of *ab initio* calculations for excitation of the $\tilde{a}\ ^3B_1$, $\tilde{A}\ ^1B_1$, $\tilde{b}\ ^3A_1$, $\tilde{B}\ ^1A_1$, $1\ ^3A_2$, and $1\ ^1A_2$ states of water by low energy electron impact. The calculations are carried out in an eight-channel close-coupling approximation using the complex Kohn variational method. Particular attention is paid to the elimination of pseudoresonances that can occur when correlated target states are employed. Differential and integral cross sections are reported and compared with the most recent experimental and theoretical results.

DOI: 10.1103/PhysRevA.88.012703 PACS number(s): 34.80.Gs

I. INTRODUCTION

There has been a resurgence of interest in the interaction of low energy electrons with water, due in large part to the key role such interactions play in understanding and modeling radiation damage in biological environments [1]. Much of the work in recent years, both experimental and theoretical, on electron-H_2O scattering has been focused on resonant collisions resulting in dissociative electron attachment [2–7]. Nonresonant dissociation, which proceeds through direct excitation of low-lying electronic states, has received relatively less attention, not because the problem is of less fundamental interest, but because it presents some formidable challenges. On the experimental side, the analysis of the electron-energy-loss spectra is complicated by the fact that the low-lying electronic states of water are dissociative and the profiles of the individual states are broad and strongly overlapped, making it difficult to extract a unique set of cross sections [8]. On the theoretical side, one is faced with the problem of coupling between a number of relatively closely spaced states that have mixed valence-Rydberg character which is difficult to capture with simple, single-configuration wave functions. Of the *ab initio* methods that have been developed for studying electron impact excitation of polyatomic molecules, only a few are capable of employing multiconfiguration target functions [9–11]. Moreover, the use of correlated target wave functions in coupled-state calculations can introduce a new set of problems associated with the appearance of unphysical pseudoresonances unless some care is taken to prevent their appearance [12].

Only a few calculations of cross sections for electronic excitation of water by electron impact have been reported. In 1990, Pritchard *et al.* [13] reported total and differential cross sections (DCS) for excitation of the $\tilde{b}\ ^3A_1$ state using the Schwinger multichannel method in a strong-coupling (two-state) approximation. These were followed several years later with distorted-wave calculations for excitation of the $\tilde{b}\ ^3A_1$ and $\tilde{d}\ ^3A_1$ states by Lee *et al.* [14,15], again using the Schwinger method to generate the distorted waves. In 1995, Gil *et al.* [16] reported total and differential cross sections for the $\tilde{a}\ ^3B_1$, $\tilde{A}\ ^1B_1$, $\tilde{b}\ ^3A_1$, and $\tilde{B}\ ^1A_1$ states from five-channel complex Kohn calculations. All of the early calculations employed single-configuration wave functions to describe the various target electronic states. The agreement among these results could only be described as fair. Moreover, the measured data on electronic excitation of water at that time was sketchy, with only two studies of electron-energy-loss spectra (EELS) by Lassettre *et al.* [17] and Trajmar *et al.* [8] that had been measured some 20 years earlier. Another piece of experimental data was provided in the 1980 study of Becker *et al.* [18] who estimated the contribution of triplet excited states to H_2O dissociation by studying OH fragment fluorescence at high electron impact energies. Morgan [19] and later Gorfinkiel, Morgan, and Tennyson [20] reported the results of *R*-matrix calculations for excitation of the same states studied by Gil *et al.* [16]. The *R*-matrix studies employed correlated target states, but unfortunately neither study reported differential cross sections. The situation with respect to electronic excitation of water was reflected in the extensive 2005 review by Itikawa and Mason [21] who found themselves unable to recommend a set of excitation cross sections.

The first set of measured absolute differential and integral cross sections for excitation of the six lowest-lying electronic states of water were reported in a series of three papers by Thorn *et al.* [22,23] and by Brunger *et al.* [24], who used an elaborate fitting procedure to unravel the contributions from the various overlapping electronic states to their measured EELS spectra. Unfortunately, the extracted cross sections were in qualitative and quantitative disagreement with the various theoretical results. The situation has changed significantly with the recent publication of new cross-section measurements and accompanying theoretical calculations by a CSU Fullerton and Caltech collaboration [25]. Much of the uncertainty in unfolding the EELS spectra was removed by using optical absorption data to fix the profiles of the allowed singlet transitions, and then subtracting their contributions from the EELS data before fitting the contributions from the remaining optically forbidden transitions. It was noted in this recently published study that the new Schwinger multichannel calculations were, with a few notable exceptions, in reasonably good agreement with the new measurements, as well as with the older calculations of Gil *et al.* [16]. These developments have prompted us to reexamine the original calculations of Gil *et al.*, employing here a larger set of states in the close-coupling expansion as well as more elaborate target wave functions. The present study is aimed at further examining the remaining discrepancies between theory and experiment.

II. THEORY

The present calculations were carried out using the complex Kohn variational method. Since the implementation of the method has been described in some detail elsewhere [9,10], we will concentrate here on aspects of the implementation relevant to the current application. The form of the trial wave function we use is common to most variational close-coupling methods, no matter how they are implemented. The full $(N+1)$-electron wave function for an electron incident on a target molecule in a state labeled by Γ_0 is written as

$$\begin{aligned}\Psi &= \sum_{\Gamma}\mathcal{A}[\Phi_\Gamma(\vec{r}_1\cdots\vec{r}_N)F_{\Gamma\Gamma_0}(\vec{r}_{N+1})] \\ &\quad + \sum_{\mu} d_\mu^{\Gamma_0}\Theta_\mu(\vec{r}_1\cdots\vec{r}_{N+1}) \\ &\equiv P\Psi + Q\Psi, \end{aligned} \tag{1}$$

where the first sum in Eq. (1) runs over the target states Φ_Γ included in the close-coupling expansion, $F_{\Gamma\Gamma_0}$ are channel functions describing the scattered electron, and $\mathcal{A}$ is the antisymmetrizer. The second sum consists of $(N+1)$-electron terms built from square integrable functions, typically described with the catchphrase correlation and polarization terms. We note that in the present context, the second sum, if unrestricted, should be labeled "Here be dragons."

For reasons of practicality when carrying out calculations on many-electron systems, the basis functions used to represent the channel functions F are generally constrained to be orthogonal to all the functions used to construct the target functions Φ. This "strong orthogonality" constraint should be relaxed in the case where open-shell target states are included in the expansion or when multiconfiguration target states with partially occupied molecular orbitals are used. These constraints are usually removed by including in $Q\Psi$ those $(N+1)$-electron configurations, or so-called "penetration" terms, that can be formed as the direct product of all N-electron target configurations and partially occupied target molecular orbitals [9].

When the number of states included in $P\Psi$ is less then the full number of configurations used in their construction, which is generally the case when a large complete-active-space (CAS) configuration-interaction calculation is used to determine the target states, then spurious resonances can arise from the inclusion of Q-space penetration terms corresponding to energetically open channels not explicitly included in $P\Psi$. Rather than including additional target states in $P\Psi$, which would be only poorly described in a limited CAS space, we can remove spurious resonances by taking only specific linear combinations of penetration terms consistent with the channels explicitly included in $P\Psi$. We call this a contraction of Q space. Technical details of how this contraction is carried out are discussed in Ref. [12]. A similar procedure was used in the context of molecular photoionization by Stratmann *et al.* [26]. Basically, the expansion of $Q\Psi$ in Eq. (1) is replaced by a smaller number of terms:

$$Q\Psi = \sum_{i,\Gamma}\left[d_{i,\Gamma}^{\Gamma_0}\mathcal{A}[\phi_i\Phi_\Gamma]\right] \equiv \sum_{i,\Gamma} d_{i,\Gamma}^{\Gamma_0}\Omega_{i,\Gamma}, \tag{2}$$

where $[\phi_i]$ is the set of orbitals used to construct the target states. The $(N+1)$-electron terms Ω will, in general, be unnormalized and nonorthogonal. To assure that $Q\Psi$ does not introduce pseudoresonances, we begin by discarding all terms Ω that have small norms, which will be the case when the electron being added in ϕ_i is close to being doubly occupied in Φ_Γ. The remaining Q-space vectors are then sequentially orthonormalized and, in the process, terms with small overlaps with the preceding vectors are also discarded. We refer the interested reader to Ref. [12] for additional details.

TABLE I. Vertical excitation energies (in eV) for low-lying states of water, comparing computed results using CI wave function, single-configuration (IVO) values, spectroscopic assignments from EELS analysis of Ref. [25], and theoretical results from Ref. [28].

State	CI	IVO	Obs.	MRCI [28]
$\tilde{a}\ ^3B_1(1b_1 \to 4a_1)$	7.46	8.05	7.20	7.14
$\tilde{A}\ ^1B_1(1b_1 \to 4a_1)$	8.15	8.78	7.41	7.81
$1\ ^3A_2(1b_1 \to 2b_2)$	9.58	10.02	8.90	9.42
$\tilde{b}\ ^3A_1(3a_1 \to 4a_1)$	9.81	10.33	9.46	9.78
$1\ ^1A_2(1b_1 \to 2b_2)$	9.84	10.38	9.20	9.30
$\tilde{d}\ ^3A_1(1b_1 \to 2b_1)$	10.22	11.26	9.79	10.52
$\tilde{b}\ ^1A_1(3a_1 \to 4a_1)$	10.37	11.66	9.67	9.78

III. COMPUTATIONS

The L^2 functions used in the present calculations were constructed from an $(11s,7p,5d)$ Gaussian basis on oxygen, contracted to $(7s,6p,5d)$, and a $(7s,4p)$ hydrogen basis, contracted to $(5s,4p)$, for a total of 89 functions. This basis is the 77 function basis used by Gil *et al.*, augmented with an additional diffuse d function on oxygen and an additional p function on the hydrogens. The active space of orbitals used to construct the target states consisted of eight functions: five (three a_1, oneb_1, and one b_1) obtained from a Hartree-Fock calculation on the ground state of H_2O and three additional orbitals ($4a_1$, $2b_1$, $2b_2$) obtained from a triplet-coupled improved virtual orbital (IVO) calculation [27] with a

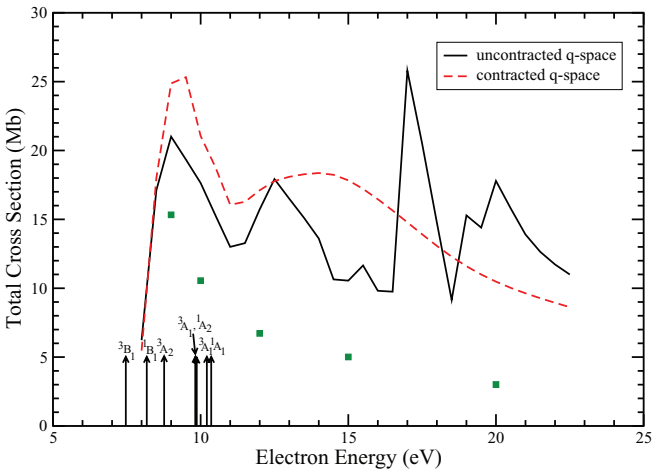

FIG. 1. (Color online) Computed total cross sections, in megabarns (Mb), for excitation of the $^3B_1$ state of water, comparing results with and without contraction of Q-space penetration terms, as discussed in text. Vertical arrows indicate calculated excitation thresholds for excited target states. 1 Mb $= 10^{-18}$ cm^2.

hole placed in the $1b_1$ orbital. The target states were generated from configuration-interaction (CI) calculations in the eight-function active space, including single, double, and triple excitations from the ground-state reference configuration, keeping the oxygen $1s$ orbital doubly occupied, which resulted in CI expansions of 60–70 terms, depending on the symmetry of the state. The variational expansion basis used to construct the channel functions F [Eq. (1) consisted of the virtual space of 81 Gaussian molecular orbitals (89 total minus the eight active space orbitals] plus numerical continuum functions up to $l = |m| = 6$.

We included the first eight electronic states of the target in our close-coupling expansion. The computed excitation energies are listed in Table I, along with experimental values deduced from the EELS spectra, values obtained from single-configuration IVO calculations, and the large-scale (MRCI + Q) results of Cai *et al.* [28]. The CI calculations are found to reduce the errors in the IVO excitation energies from a minimum of 0.44 eV to a maximum of 1.2 eV, depending on the transition.

The Q-space terms in the present calculations only included penetration terms generated from the direct product of target orbitals (excluding the doubly occupied $1a_1$ orbital) and the N-electron terms used in the CI target state calculations. However, before these terms were folded into an optical potential, they were contracted according to the procedure outlined in the previous section. The variational complex Kohn equations were then solved in the usual manner to calculate the excitation cross sections.

We note that the $X\,^1A_1 \rightarrow \tilde{A}\,^1B_1$ and $X\,^1A_1 \rightarrow \tilde{B}\,^1A_1$ transitions are optically allowed. To properly describe the magnitude and characteristically forward peaked DCS for these cases, it is important to account for the long-range transition dipole interaction associated with these excitations. We computed the transition dipole moments for these two cases and used them in a Born-closure procedure, as described previously [29], that properly incorporates these long-range effects in the computed cross sections.

IV. RESULTS

As discussed above, a common prescription for carrying out close-coupling expansions with correlated target states is to impose a strong orthogonality condition on the channel functions which is then relaxed through the inclusion of $(N + 1)$ -electron penetration terms into the total wave function. The

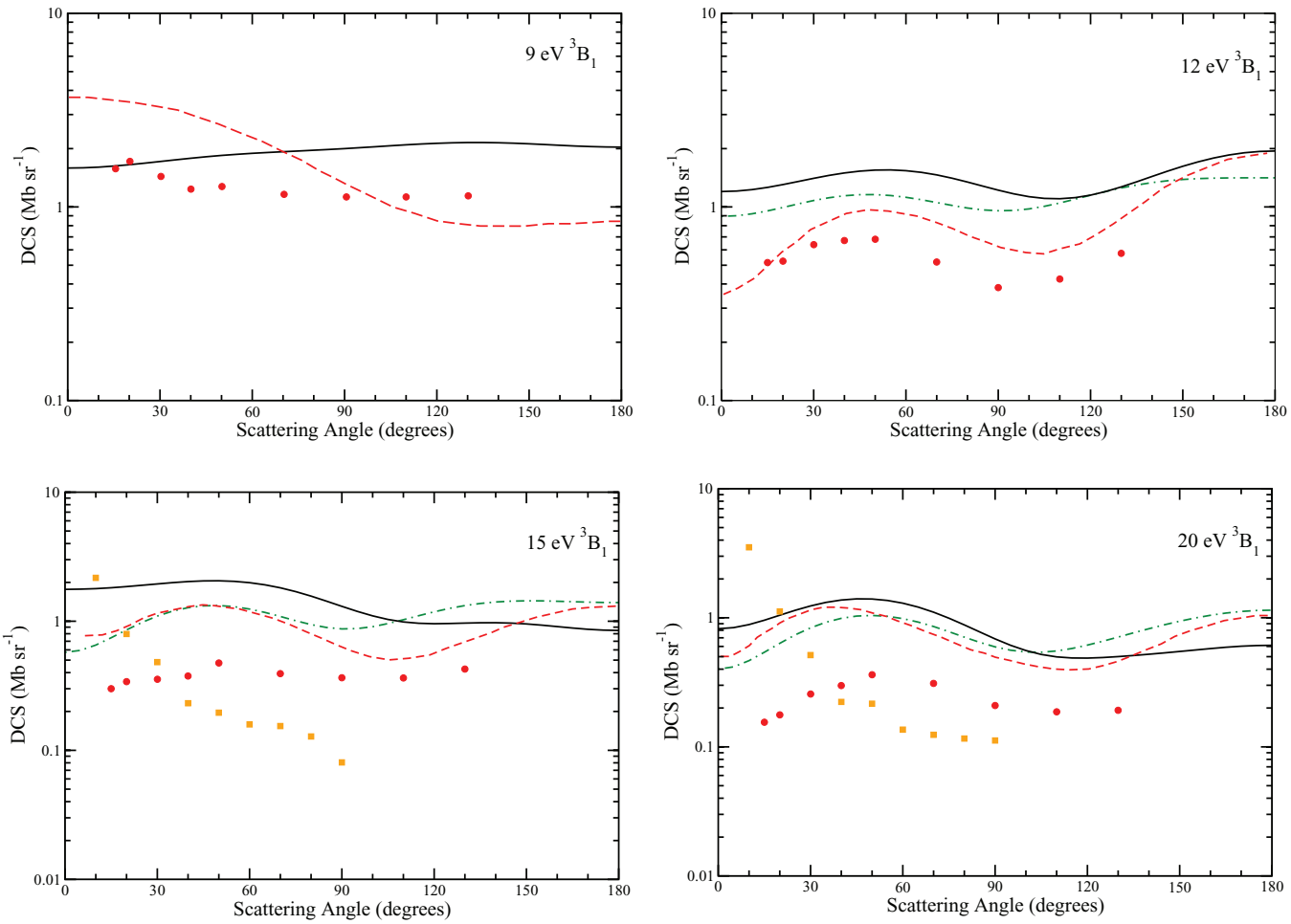

FIG. 2. (Color online) Differential cross sections for excitation of the $^3B_1$ state of water at 9, 12, 15, and 20 eV. Solid curves, present results; dashed curves, Schwinger multichannel results from Ref. [25]; dash-dotted curves, complex Kohn results of Gil *et al.*; circles, experimental results of Ralphs *et al.*; squares, experimental results of Thorn *et al.*

problems that can ensue with the use of multiconfiguraton target functions in a limited close-coupling expansion is illustrated in Fig. 1, where we show calculated total cross sections for excitation of the $^3B_1$ state with and without implementing the Q-space contraction discussed above. For clarity, the energies of the target electronic states are indicated in the figure. The use of an uncontracted Q space results in unphysical features in the cross section, which are clearly unrelated to the target state thresholds. These disappear when the Q space of penetration terms is properly contracted. We note that the peak in the total cross section near 10 eV, which is present in both contracted and uncontracted results, is physical and is associated with a doubly excited $^2A_1$ Feshbach resonance [16]. All the results reported in what follows were obtained after contracting Q space.

A. Differential cross sections

Our calculated DCS are plotted in Figs. 2–5, where they are compared with the earlier complex Kohn results of Gil *et al.* [16], the measurements and accompanying Schwinger multichannel results of Ralphs *et al.* [25], and the earlier measurements of Thorn *et al.* [22–24].

For the $^3B_1$ state, the theoretical results are all in qualitative agreement with each other and with the measurements of Ralphs *et al.*, except at 9 eV. The present results, however, are somewhat larger in magnitude than the other theoretical results, which we suspect may be more related to our use of correlated target states here than to differences in the number of states that were included in the calculations. Results for the $^1B_1$ state support this conclusion. The DCS for this case display the characteristic forward peaking expected for an optically allowed transition. One might expect that the larger values of the present DCS results in the forward direction might be directly related to the magnitude of the computed transition dipole moment, but this proves not to be the case. Indeed, our present CI treatment and the earlier single-configuratiion IVO treatment of the electronic states both give transition dipole moments for the $X\ ^1A_1 \rightarrow \tilde{A}\ ^1B_1$ very close to 0.5 atomic units. We conclude that the small-angle DCS are sensitive to the increased valence character of the excited state, which couples more strongly to the initial state, when correlated target states are used.

The qualitative disagreement with experiment at 9 eV for both $^3B_1$ and $^1B_1$ states may be related to the inevitable breakdown of the Franck-Condon assumptions in both the calculations, all carried out at a single fixed-nuclear geometry, as well as in the analysis of the EELS spectra, which assumes equivalence of the optical absorption and electron excitation profiles for the optically allowed transitions, as one approaches

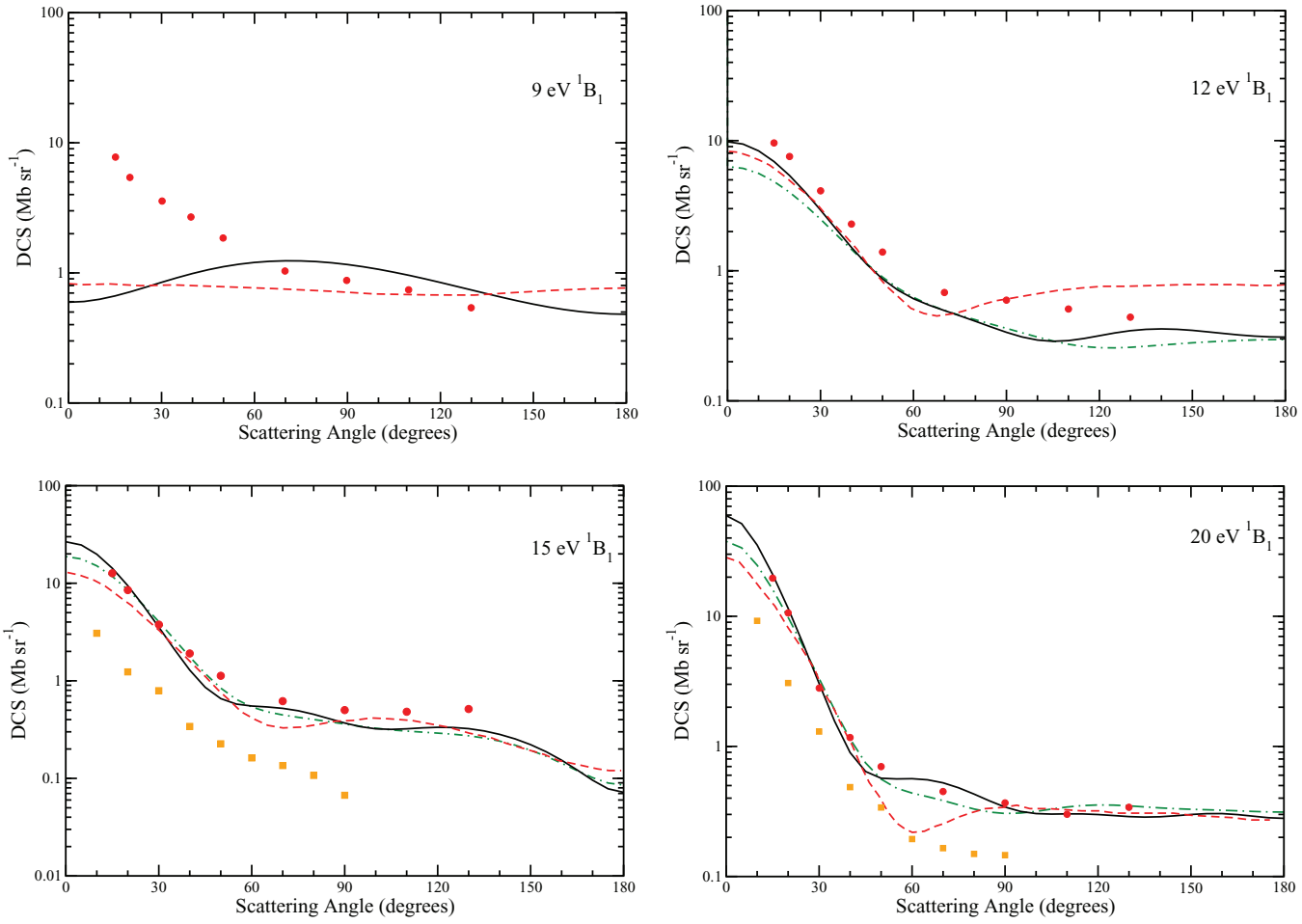

FIG. 3. (Color online) As in Fig. 2, for the $^1B_1$ state.

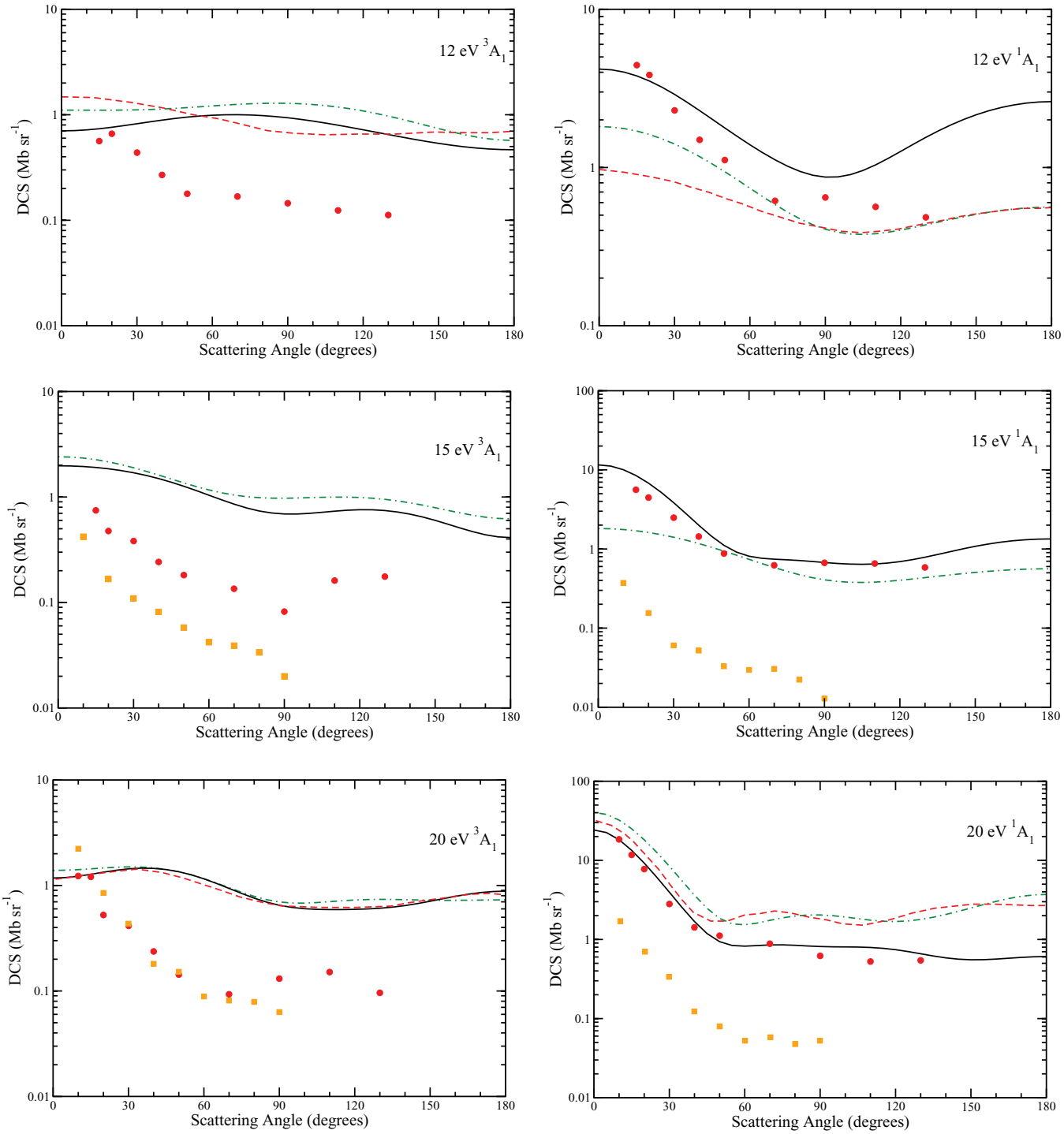

FIG. 4. (Color online) As in Fig. 2, for the $^3A_1$ and $^1A_1$ states.

threshold. Ralphs *et al.* have commented on the qualitative disagreement between their new measurement, as well as theory, and the earlier results of Thorn *et al.* for the $^3B_1$ excitation DCS. The analysis performed by the latter shows evidence of contamination in the $^3B_1$ excitation DCS due to incomplete subtraction of overlapping $^1B_1$ state contributions.

For the optically forbidden $^3A_1$ state, there is uniformly good agreement among all the theoretical calculations. All the calculations, however, give cross sections that are significantly larger in magnitude than the measured values. The situation is much improved in the case of the allowed $^1A_1$, when the present calculations are in excellent agreement with the measurements of Ralphs *et al.* Agreement between the various calculations is reasonable, with the largest differences seen in the magnitude of the DCS at small angles. It has been noted that the $(3a_14a_1)^1A_1$ state has a mixed valence-Rydberg character which is difficult to describe with a single-configuration wave function, as it is sensitive to the coupling scheme used

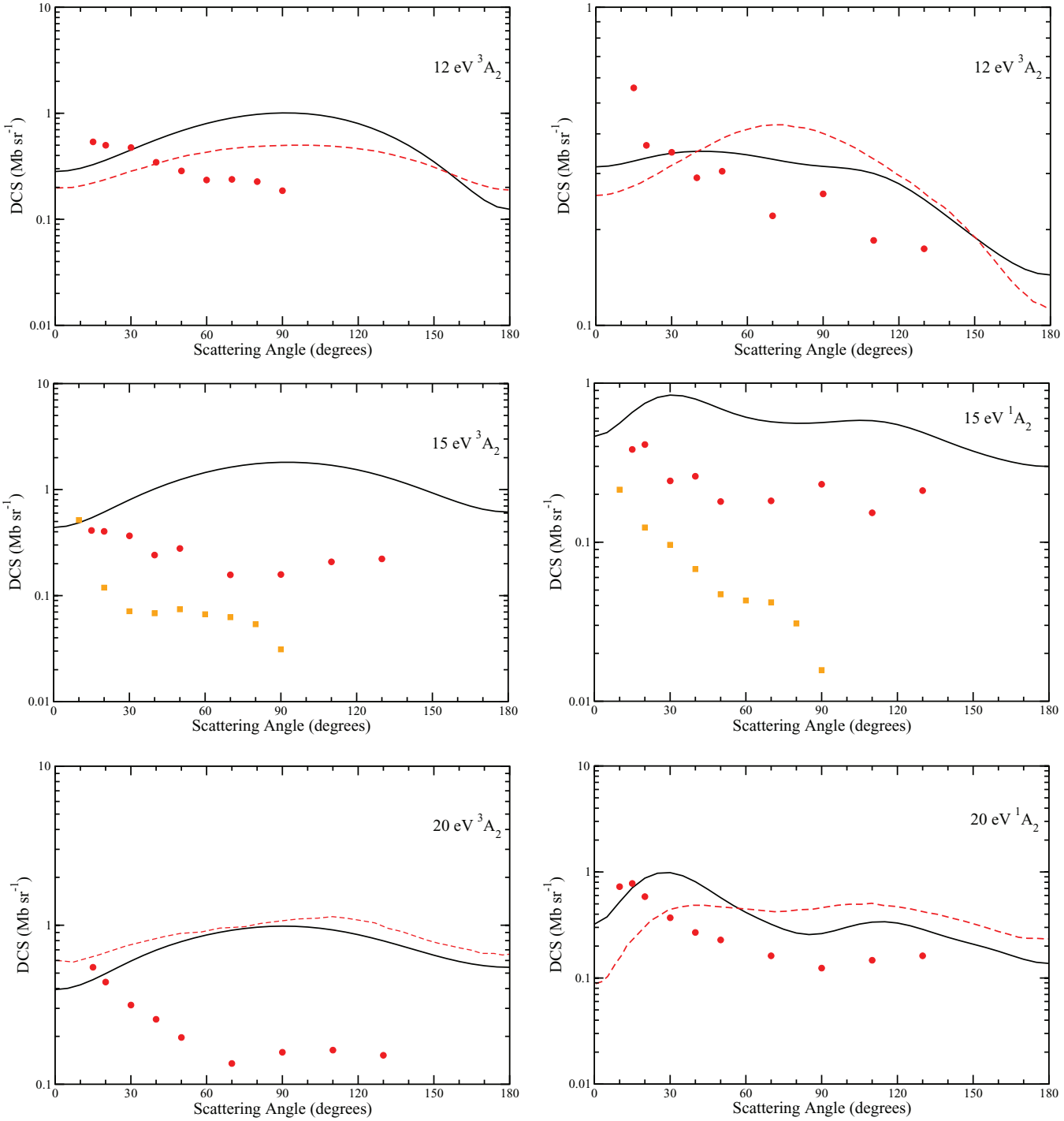

FIG. 5. (Color online) As in Fig. 2, for the $^3A_2$ and $^1A_2$ states.

to generate the $4a_1$ orbital [16]. With single-configuration functions in the triplet-coupled IVO scheme employed in Gil *et al.* and Ralphs *et al.*, the transition dipole moment for this state is 0.76 a.u., whereas the value we obtained with CI wave functions is 0.50 a.u., indicating a slightly more Rydberg character for this state.

Our results for the $^3A_2$ and $^1A_2$ state DCS agree well with the multichannel Schwinger results of Ralphs *et al.* As they have noted, the fact that the DCS have minima at 0° and 180°, in evident disagreement with the measurements, is to be expected on theoretical grounds. An atomic selection rule, which in this case is only a propensity rule, explains the behavior. For the "parity unfavored" electron-impact excitation $1s^2\,{}^1S \rightarrow 2p^2\,{}^3P^e$ in He, Becker and Dahler first predicted [30], and Fano later explained [31] why the DCS vanished in the forward and backward directions. In the present case of water, the $^{1,3}A_2$ states are well described by the configuration $(1b_1 2b_2)$. The $1b_1$ orbital in water is the oxygen lone pair $(2p_x)$ which is atomiclike, while the$2b_2$ orbital is a Rydberg-like $3p_y$ orbital, so the analogy with He $(2p_x 2p_y)\,{}^3P^e$ explains the propensity

rule. As for the disagreement with experimentally derived DCS for these cases, we note that the $^{1,3}A_2$ states are buried under the strongly overlapping $^3A_1$ and $^1A_1$ states in the EELS spectrum, so the cross sections derived from the measurements may suffer from nonuniqueness in the fitting procedure, as discussed by Ralphs *et al.* It is worth mentioning that in the work of Ralphs *et al.*, the $^{1,3}A_2$ states were assumed to be dissociative. This is a curious assertion, given the fact that these states are Rydberg in nature and that the water monocation is bound. Indeed, in varying the nuclear geometry, we found these states to be nondissociative. The *R*-matrix calculations of Gorfinkiel *et al.* [20] also show these states to be bound. It is possible that this may have some bearing on the way the unfolding of the EELS data was carried out.

B. Integral cross sections

Integral cross sections for the aforementioned transitions are given in Figs. 6–8. In addition to the previous Schwinger and Kohn results, we have also included the results from the earlier *R*-matrix calculations [19,20] for comparison. The *R*-matrix studies, like the present calculations, also employed correlated target states, but the $(N+1)$-electron correlation and polarization terms (Q-space terms in our parlance) were included without contraction.

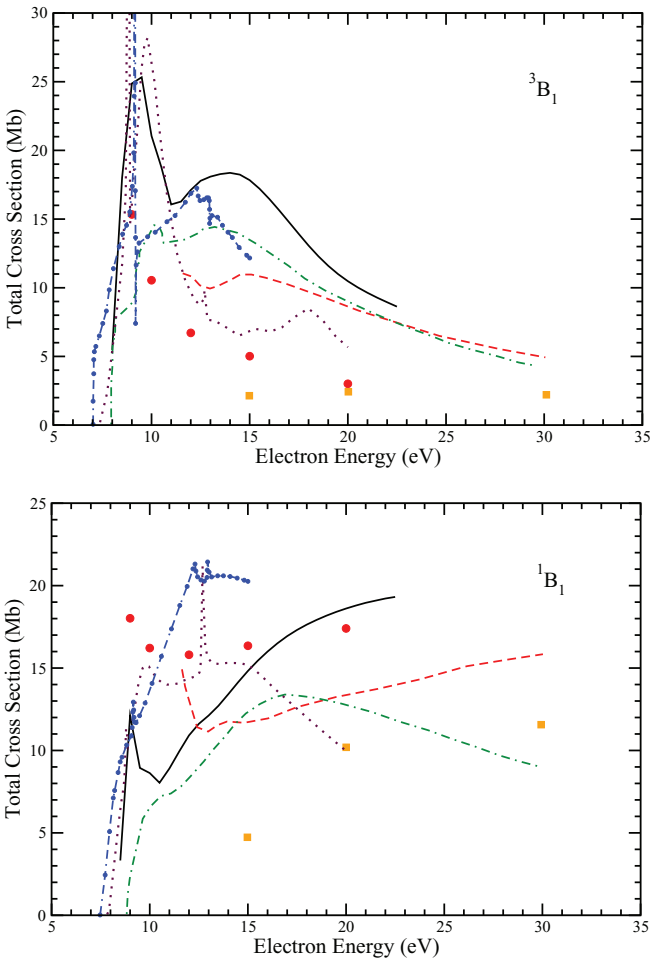

FIG. 6. (Color online) Total excitation cross sections for the $^3B_1$ and $^1B_1$ states of water. Dotted curves, *R*-matrix results of Morgan [19]; chained curve with circles, nine-state *R*-matrix results of Gorfinkiel *et al.* [20]. Legend for other results as in Fig. 2.

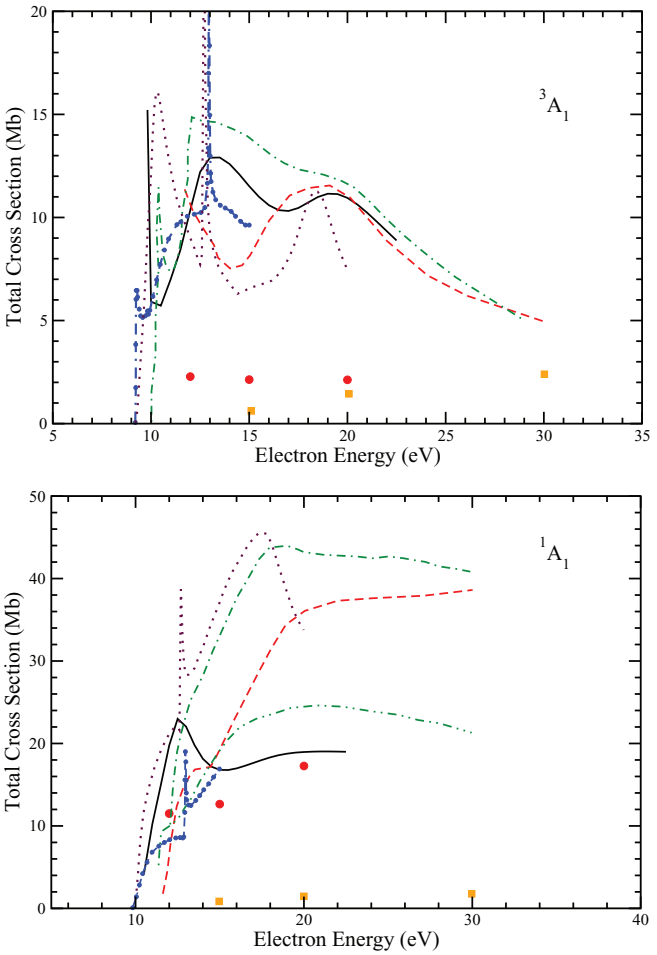

FIG. 7. (Color online) As in Fig. 6, for the $^3A_1$ and $^1A_1$ states of water. For $^1A_1$ excitation cross section, the dash-dot-dot-dashed curve is the result of Gil *et al.* when singlet coupling was used to generate the $4a_1$ IVO orbital (see text).

For the $^3B_1$ state, our calculated cross sections are somewhat higher than the values reported in the earlier complex Kohn and multichannel Schwinger studies. We believe the differences to be primarily due to our use of correlated target states, which gives a more compact description of the excited states in question that have better spatial overlap with the initial state and hence larger excitation cross sections. Another significant difference between the current and earlier results is the broad peak we find centered near 10 eV. Of the earlier calculations, only the *R*-matrix calculations of Morgan, which coincidently employed the same Gaussian basis used by Gil *et al.*, show a similar behavior near 10 eV. Gorfinkiel *et al.* believed this peak to be an artifact caused by Morgan's use of diffuse target basis functions that extended beyond the *R*-matrix box, so in their calculations, the diffuse functions were deleted. Their results, while in relatively good agreement with ours above 12 eV, show no broad 10 eV peak. The use of diffuse functions is not precluded in the complex Kohn method. We therefore conclude that to properly describe the excitation cross section in this channel below 12 eV, we need a correlated target excited

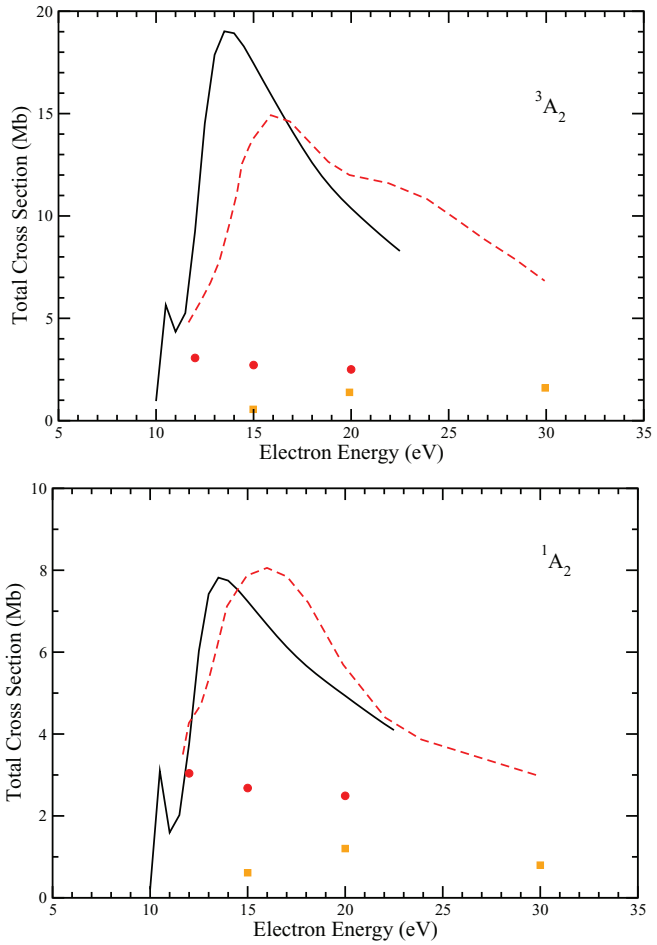

FIG. 8. (Color online) As in Fig. 6, for the $^3A_2$ and $^1A_2$ states of water.

state computed in a basis with enough diffuse functions to properly represent its spatial extent.

For the $^1B_1$ state, all of the theoretical results show a similar energy dependence and agree in magnitude by roughly a factor of 2. The agreement with the experimental results of Ralphs *et al.* is also reasonably good for this predominately valencelike, optically allowed state.

There is little agreement between theory and experiment for the $^{1,3}A_2$ states, for the reasons discussed above. It is noteworthy that the agreement between the complex Kohn and multichannel Schwinger calculations for these cases is excellent. The $^{1,3}A_2$ states were included as target states in the *R*-matrix calculations of Morgan and in the nine-state calculations of Gorfinkiel *et al.*, but in neither study were cross sections reported for these states, because of their Rydberg character.

There is general agreement the among the theoretical results in the magnitudes of the $^3A_1$ cross sections, all of which are substantially larger than the measured values. The present calculation, like those of Gil *et al.* and Gorfinkiel *et al.*, show a broad peak centered near 13 eV, while in the multichannel Schwinger results and in the *R*-matrix results of Morgan, the cross-section peak appears several eV lower in energy.

The $^1A_1$ cross section has an energy dependence similar to the $^1B_1$ cross section, although there is a greater spread among the theoretical results for this case. We have noted above that the mixed valence-Rydberg character of the $^1A_1$ state is particularly difficult to capture in a single-configuration target function. The Schwinger calculations, like those of Gil *et al.* obtained with a triplet-coupled $4a_1$ IVO orbital, produce relatively large cross sections above 15 eV. Significantly, Gil *et al.* found the cross sections to drop by a factor of 2 when singlet coupling was used to generate the $4a_1$ orbital, giving results in much better agreement with what we find here, as well as with the results of Gorfinkiel *et al.* It seems likely that the triplet-coupled IVO treatment exaggerates the valence character of the final state, which is more properly described with a correlated wave function. Our results agree well with the measurements of Ralphs *et al.*, but this agreement may be fortuitous.

V. CONCLUSIONS

While the agreement between theory and experiment is much improved with the appearance of the recent measurements of Ralphs *et al.*, the agreement is only moderate is some cases, and poor in others. The present calculations have attempted to improve on earlier complex Kohn and multichannel Schwinger results for electron-impact excitation of water by using a set of correlated target states in the coupled-channel expansion. This is particularly important when considering excited states that have mixed valence-Rydberg character which is difficult to properly describe with single-configuration target functions. We have shown that, with moderately sized close-coupling expansions, spurious pseudoresonances can arise at energies far from physical thresholds, but that an appropriate contraction of the so-called penetration terms can be performed which removes these pseudoresonances without imposing a strong orthogonality constraint between target and scattering wave functions.

There is clearly more work that needs to be done, both theoretically and experimentally, to better determine a set of excitation cross sections for water. On the theory side, the effects of varying the nuclear geometry away from its equilibrium value need to be investigated, so that the profiles of the dissociative excitation cross sections can be obtained and used to test the accuracy of the Franck-Condon approximation, whose validity is assumed when using optical absorption profiles to assist in the analysis of the electron-impact measurements. Such studies might aid in unfolding the EELS spectra where broadly overlapping contributions from a number of different states makes it difficult to extract a unique set of cross sections.

ACKNOWLEDGMENTS

This work was performed under the auspices of the US Department of Energy by the University of California Lawrence Berkeley National Laboratory under Contract No. DE-AC02-05CH11231 and was supported by the US DOE Office of Basic Energy Sciences, Division of Chemical Sciences. A.E.O. acknowledges support by the National Science Foundation, with some of this material based on work while serving at NSF.

[1] B. C. Garrett *et al.*, Chem. Rev. **105**, 355 (2005).
[2] J. Fedor, P. Cicman, B. Coupier, S. Feil, M. Winkler, K. Gluch, J. Husarik, D. Jaksch, B. Farizon, N. J. Mason *et al.*, J. Phys. B **39**, 3935 (2006).
[3] D. J. Haxton, C. W. McCurdy, and T. N. Rescigno, Phys. Rev. A **75**, 012710 (2007).
[4] D. J. Haxton, T. N. Rescigno, and C. W. McCurdy, Phys. Rev. A **75**, 012711 (2007).
[5] E. Krishnakumar, V. S. Prabhudesai, and N. B. Ram, J. Phys.: Conf. Ser. **88**, 012073 (2007).
[6] D. J. Haxton, T. N. Rescigno, and C. W. McCurdy, Phys. Rev. A **78**, 040702 (2008).
[7] H. Adaniya, B. Rudek, T. Osipov, D. J. Haxton, T. Weber, T. N. Rescigno, C. W. McCurdy, and A. Belkacem, Phys. Rev. Lett. **103**, 233201 (2009).
[8] S. Trajmar, W. Williams, and A. Kuppermann, J. Chem. Phys. **58**, 2521 (1973).
[9] T. N. Rescigno, B. H. Lengsfield, and C. W. McCurdy, *Modern Electronic Structure Theory* (World Scientific, Singapore, 1995), Vol. 1.
[10] T. N. Rescigno, C. W. McCurdy, A. E. Orel, and B. H. Lengsfield III, *Computational Methods for Electron-Molecule Collisions* (Plenum, New York, 1995).
[11] L. A. Morgan, J. Tennyson, and C. J. Gillan, Comput. Phys. Commun. **114**, 120 (1998).
[12] B. H. Lengsfield and T. N. Rescigno, Phys. Rev. A **44**, 2913 (1991).
[13] H. P. Pritchard, V. McKoy, and M. A. P. Lima, Phys. Rev. A **41**, 546(R) (1990).
[14] M. T. Lee, S. E. Michelin, and L. M. Brescansin, J. Phys. B **26**, L203 (1993).
[15] M. T. Lee, S. E. Michelin, T. Kroin, L. E. Machado, and L. M. Brescansin, J. Phys. B **28**, 1859 (1995).
[16] T. J. Gil, T. N. Rescigno, C. W. McCurdy, and B. H. Lengsfield III, Phys. Rev. A **49**, 2642 (1994).
[17] E. N. Lassetre, A. Skerbele, M. A. Dillon, and K. J. Ross, J. Chem. Phys. **21**, 145 (1968).
[18] K. Becker, B. Stompf, and G. Schulz, Chem. Phys. Lett. **73**, 102 (1980).
[19] L. A. Morgan, J. Phys. B **31**, 5003 (1998).
[20] J. D. Gorfinkiel, L. A. Morgan, and J. Tennyson, J. Phys. B **35**, 543 (2002).
[21] Y. Itikawa and N. Mason, J. Phys. Chem. Ref. Data **34**, 1 (2005).
[22] P. A. Thorn *et al.*, J. Chem. Phys. **126**, 064306 (2007).
[23] P. A. Thorn, M. J. Brunger, H. Kato, M. Hoshino, and H. Tanaka, J. Phys. B **40**, 697 (2007).
[24] M. J. Brunger *et al.*, Int. J. Mass Spectrom. **271**, 80 (2008).
[25] K. Ralphs, G. Serna, L. R. Hargreaves, M. A. Khakoo, C. Winstead, and V. McKoy, J. Phys. B **46**, 125201 (2013).
[26] R. E. Stratmann, R. W. Zurales, and R. R. Lucchese, J. Chem. Phys. **104**, 8989 (1996).
[27] W. J. Hunt and W. A. Goddard III, Chem. Phys. Lett. **3**, 414 (1969).
[28] Z. L. Cai, D. J. Tozer, and J. R. Reimers, J. Chem. Phys. **113**, 7084 (2000).
[29] T. N. Rescigno and B. I. Schneider, Phys. Rev. A **45**, 2894 (1992).
[30] P. M. Becker and J. S. Dahler, Phys. Rev. Lett. **10**, 491 (1963).
[31] U. Fano, Phys. Rev. **135**, B863 (1964).